University of Dundee

Dynamics of human facial aging through photoanthropometric analysis and quadratic modeling from child- to adulthood – a multi-centric study

Lima, Laíse Nascimento Correia; Santiago, Bianca Marques; Franco, Ademir; Thevissen, Patrick; Vidal, Flávio De Barros; Porto, Lucas Faria

Dynamics of human facial aging through photoanthropometric analysis and quadratic modeling from child- to adulthood – a multi-centric study

Laíse Nascimento Correia Lima*,******** PhD; Bianca Marques Santiago**,********* PhD;
Ademir Franco***,**** PhD; Patrick Thevissen**** PhD; Flávio de Barros Vidal***** PhD;
Lucas Faria Porto***** MSc; Inmaculada Aleman Aguilera****** PhD;
Carlos Eduardo Palhares Machado******* PhD; Eduardo Daruge Jr* PhD

Abstract

This study aimed to investigate the dynamics of facial aging from photographs of individuals in different age groups and establish a pattern of facial growth. The sample consisted of digital photographs standardly taken from 1273 Brazilians aged between 2 and 24 years and equally distributed by sex into 12 specific age groups (2, 4, 6, 8, 10, 12, 14, 16, 18, 20, 22 and 24 years). SAFF-2D® (Forensic Facial Analysis System, Brazilian Federal Police, Brazil) software package was used for positioning 28 landmarks on each photograph. Two-hundred and eight measurements were established between the landmarks. Photoanthropometric Indicators (PAI) of facial morphological alterations were obtained from the relations of facial measurements with a fixed reference (diameter of the iris). Non-transformed linear, quadratic and log-linear models were tested to screen the best approach to describe the facial growth with aging in females and males. The quadratic model reached the best outcomes in females (R^2 <73.2%, mean: 52.14% ± 0.15) and males (R^2 <80.8%, mean: 60.87% ± 0.15). Most of the PAI (>99.04%) were statistically associated with age in females and males ($p < 0.05$). Vertical facial alterations were

* Departamento de Odontologia Legal, Faculdade de Odontologia de Piracicaba, Universidade Estadual de Campinas, Av. Limeira 901, 13.414-903, Piracicaba, Brasil

** Departamento de Odontologia Clínica e Social, Universidade Federal da Paraíba. Campus I, Cidade Universitária, 58.051-900, João Pessoa, Brasil.

*** Department of Imaging and Pathology, Forensic Odontology, KU Leuven. Kapucijnenvoer 7, block B, 3000, Leuven, Belgium.

**** Division of Oral Radiology, Faculdade São Leopoldo Mandic, Instituto de Pesquisas São Leopoldo Mandic, Rua José Rocha Junqueira 13, 13.045-755, Campinas, Brasil.

***** Departamento de Ciências da Computação, Universidade de Brasília. Campus Darcy Ribeiro, Asa Norte, 70.910-900, Brasília, Brasil.

****** Departamento de Medicina Legal, Toxicología y Antropología Física, Universidad de Granada, Spain. Av. de la Investigación 11, 18.016, Granada, España.

******* Instituto Nacional de Criminalística, Polícia Federal Brasileira. Setor Policial, Quadra 7, Lote 23, Asa Sul, 70.610-200, Brasília, Brasil.

******** Departamento de Odontologia, Universidade Federal do Maranhão. Av. dos Portugueses s/n, Bacanga, 65.080-805, São Luiz, Brasil.

********* Departamento de Medicina e Odontologia Legal, Polícia Científica da Paraíba. R. Rua Antônio Teotônio s/n, Cristo Redentor, 58.071-620, João Pessoa, Brasil.

the most evident over the time, especially the height of the human face (p<0.05). Data extraction and treatment performed with the photoanthropometric analysis and the quadratic statistical model described the dynamics of human facial growth aging from child- to adulthood. These outcomes may support clinicians in treatment planning and follow-up of interventions that prevent and intercept changes in the human face.

Keywords: Aging; Anatomy; Anthropology; Forensic medicine; Forensic dentistry

Introduction

Studies in facial growth and anatomy are fundamental to support optimal performances in health (RAFAI *et al*., 2016) and forensic sciences (LINDSAY, RÜHLI, DELEON, 2015; ERICKSON *et al*., 2017). In the first, knowledge of the facial morphological structures is necessary to guide maxillofacial surgeries (e.g. orthognatic surgery, cleft lip and palate reconstructions, and traumatology) and orthodontic treatment (e.g. prediction of development) (BISHARA, 2000). In the second, simulations of facial age progression may be performed to support criminal investigations on kidnapping, illegal adoption and sexual abuse (ENLOW, 1990; LAMPINEN *et al.,* 2012; ZENG; MA; ZHOU, 2019)

Facial morphology considerably changes from child to adulthood (ENLOW, 1990; TAYLOR, 2000; WILKINSON; RYNN, 2012; XU *et al*., 2019) in a dynamic and continuous process guided by timing (ENLOW, 1990; RICANEK; BOONE,

2005; SCANDRETT; SOLOMON; GIBSON, 2006; RIGHI; PEISSIG; TARR, 2012; ERICKSON *et al*., 2017). In this process, the human face does not change uniformly (ENLOW, 1990; TURK; PENTLAND, 1991; VALENTINE, 2001; RICANEK; BOONE, 2005; KOUDELOVA *et al*., 2015). In practice, the complex allometric development of the face requires scientific strategies to study and understand the morphological changes with aging (MOREVITZ; COLLS, 2016).

Several methods are available to simulate facial aging. Many of them are founded on photographic references and on expert's knowledge of craniofacial development (TAYLOR, 2000; WILKINSON; RYNN, 2012; MOREVITZ; COLLS, 2016). The last is based on typical anthropometric models from the development of children and adolescents throughout age (ENLOW, 1990). These models may be applied in practice to update the known contemporary photograph of a person and to predict the inherent facial alterations in the future (TAYLOR, 2000). For more accurate performances in practice, the available methods proposed in the literature must be scientifically validated and new methods must be designed (CHARMAN; CAROL, 2012; ENLOW, 1990; FLORES; MACHADO, 2017).

In this scenario, photoanthropometry emerges as a promising method for the study of facial anatomy. This method consists in the bidimensional analysis of measurements, angles and proportions of human anthropological features from photographs guided by

anatomically positioned landmarks (DAVIS; VALENTINE; DAVIS, 2010; ISÇAN; HELMER, 1993; KLEINBERG; VANEZIS; BURTON, 2007; MORETON; MORLEY, 2011). As most of the facial photographs are usually taken without scales, the photoanthropometric analysis may be performed by associating the ratio of two measurements and their unification in a single index (BORGES *et al.*, 2018; FLORES *et al.*, 2019; MACHADO *et al.*, 2017). Despite the potential usefulness of photoanthropometry in anatomy highlighted by previous studies (CATTANEO *et al.*, 2009; CATTANEO *et al.*, 2012; RATNAYAKE *et al.*, 2014; TEMPORINI, 2012), the scientific literature is scarce of population-based investigations and protocols to quantify facial age progression.

This study aimed to assess facial development in Brazilian individuals through photoanthropometric analysis and to establish a morphological growth pattern as reference for estimating the development of the different anatomic structures of the human face in function of age.

Material and methods

Study design and ethical aspects

An observational cross-sectional study was designed according to the checklist described in "Strengthening the Reporting of Observational Studies in Epidemiology" (STROBE) guidelines (VON ELM *et al.*, 2008). The study was conducted after the approval of the university Committee of Ethics in Human Research – under the protocol number: 17017213.0.0000.5440.

Settings and participants

The data sample consisted of 1273 digital photographs from Caucasian Brazilians aged between 2 and 24 years. This age interval includes children and subadults up to the limit of young adulthood – covering the period of remarkable changes in the human face from a progressive aging process. The rationale behind this strategy aimed to deliver outcomes that are more applicable to practice (e.g. preventive orthopedic treatment and corrective surgical approach). The images were randomly and retrospectively collected from a national police database as an expanded sample of a previous study (MACHADO *et al.*, 2017). Image acquisition was performed in frontal view following the protocol of the International Civil Aviation Organization (ICAO), which establishes a face-camera distance of 1.5 meters and the use of standard camera, lenses and flash (BICALHO *et al.*, 2018). The obtained images were stored in .png format, 24-bit per pixel and 640x480 pixels spatial resolution. The photographs were homogeneously distributed by sex into 12 age groups (2, 4, 6, 8, 10, 12, 14, 16, 18, 20, 22 and 24, ± 1 month). Each of the age groups was composed by at least 50 photographs of males and 50 of females.

The inclusion criteria consisted of Brazilians within the age range of 2-24

years, with neutral facial expression, closed lips and face positioned directly towards the camera. The exclusion criteria consisted of individuals with evident head rotation in the sagittal, axial or coronal planes; as well individuals with evident facial deformities, asymmetries, facial hair, jewelry, make up or those with incomplete photographic registration of the face.

Data measurements and quantitative variables

The anthropometric analysis was performed by placing 28 pre-established anatomic landmarks on the human face (Table 1, Figure 1). The landmarks were placed by 10 examiners previously trained and experienced in the field. Landmark placing was feasible with SAFF-2D® (Forensic Facial Analysis System, Brazilian Federal Police, Brazil) software package, which digitally registered the landmarks as Cartesian coordinates in x- and y-axes, and horizontal and vertical axes, respectively. Two-hundred and eight measurements were obtained between each landmark. In case of bilateral measurements, the mean value between the left and right sides was considered (Figure 2).

Table 1: Description of the cephalometric landmarks used in this study

Landmark	Description
1. Nasion (n)	The interception of the midsagittal plane and the line crossing the superior palpebral creases
2. Subnasale (sn)	The lowest point of the nose on the midsagittal plane
3. Gnathion (gn)	The lowest point of the chin, on the midsagittal plane
4. Endocanthion (en)	The medial limit of the eye
5. Ectocanthion (ec)	The lateral limit of the eye
6. Iridion laterale (il)	The most lateral point of the rim of the iris
7. Iridion mediale (im)	The most medial point of the rim of the iris
8. Pupil (pu)	The central point of the iris, mathematically calculated, between the Iridion laterale and the Iridion mediale of each eye
9. Zygion (zy)	The widest point in the region of the zygomatic bone seen in the frontal view
10. Chelion (ch)	The lateral limit of the mouth
11. Alare (al)	The most lateral point on the "wing" of the nose
12. Glabella (g)	Most anterior midline point on the forehead, in the region of the superciliary ridges
13. Labiale superius (ls)	Midpoint of the vermilion border of the upper lip
14. Stomion (sto)	Midline point of the labial fissure when the lips are closed naturally, with teeth shut in the natural position
15. Labiale inferius (li)	Midpoint of the vermilion border of the lower lip
16. Midnasal (mid)	Median point at the between the endocanthion points
17. Gonion (go)	Most lateral point on the mandibular angle
18. Crista philtri (cph)	Point on each elevated margin of the philtrum just before projection to the vermilion line

Figure 1: Landmarks adopted in this study

Legend: 1. Glabella (g); 2. Nasion (n); 3. Subnasale (sn); 4. Labiale superius (ls); 5. Stomion (sto); 6. Labiale inferius (li); 7. Gnathion (gn); 8. Midnasal Ec (mid); 9. Entocanthion (en); 10. Exocanthion (ec); 11. Iridion laterale (il); 12. Iridion mediale (im); 13. Pupil (pu); 14. Zygion (zy); 15. Alare (al); 16. Gonion (go); 17. Cheilion (ch); 18. Crista philtri (cph). Morphological descriptions of these landmarks are found in Table 1.

Figure 2 – Facial measurements calculated from frontal photographs using single (A) and bilateral landmarks (B)
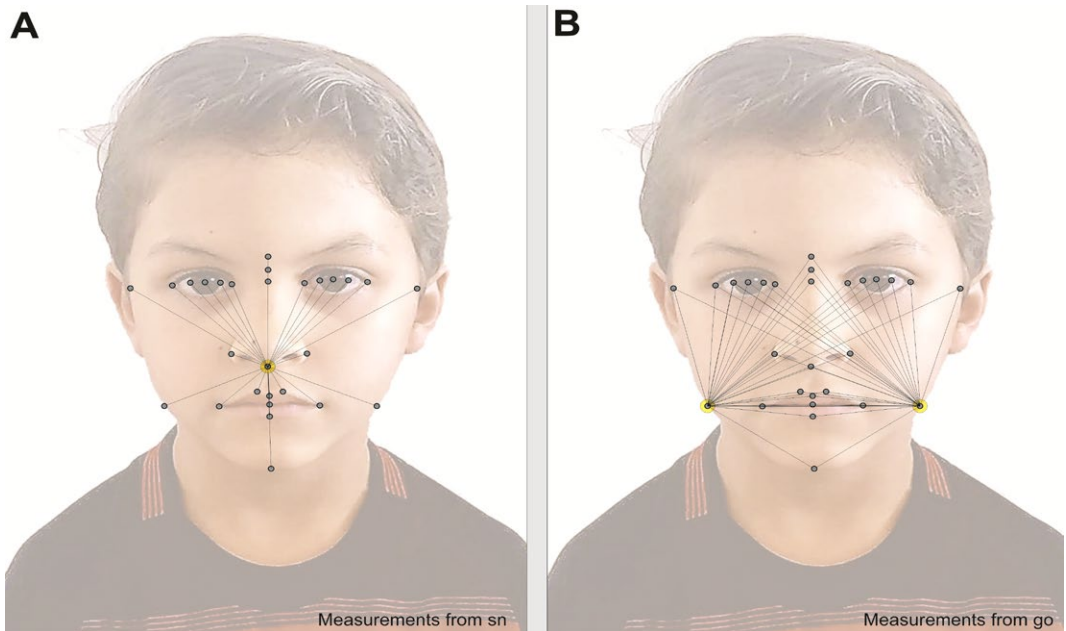
Legend: Measurements calculated from the subnasale (sn) and gonion (go) landmarks

For the analysis of facial growth, specific Photoanthropometric Indicators (PAI) were calculated from the relation of each facial measurement and the diameter of the iris. This procedure enabled the analysis of facial growth as function of age using the diameter of the iris as the most stable calibration reference in the human face (MACHADO et al., 2017).

Assessment of examiner bias

Intra- and inter-examiner bias was assessed by randomly selecting 10 photographs and providing them for landmark placement. This subsample was analyzed three times by each of the examiners within an interval of 15 days between the analyses. The reproducibility between examiners was expressed within the Intraclass Correlation Coefficient.
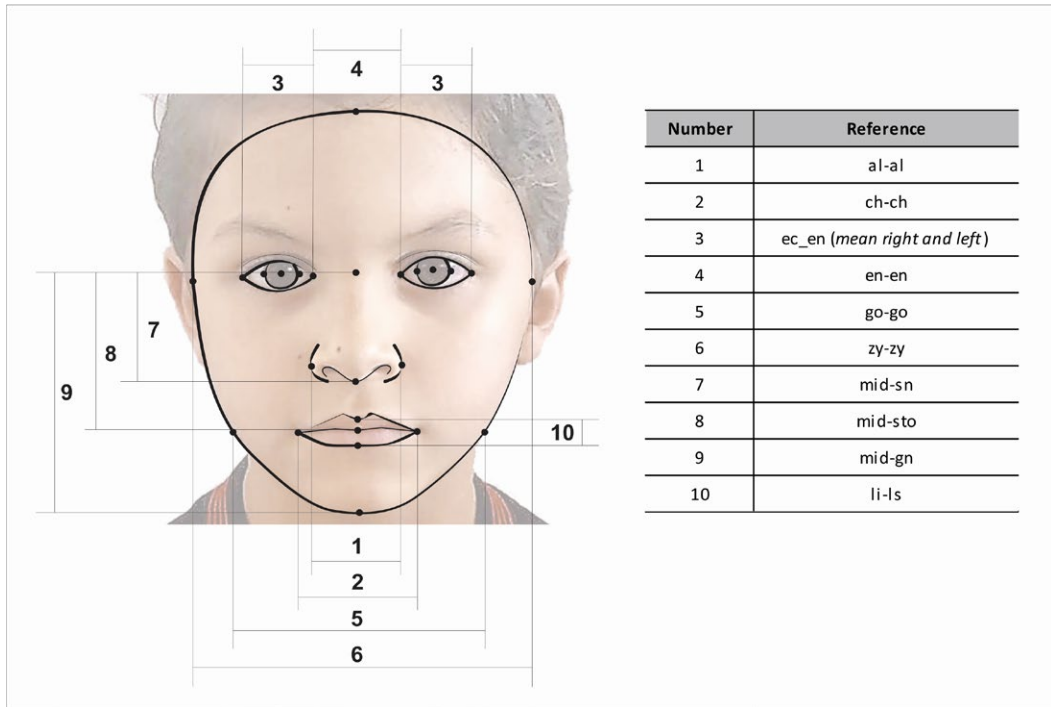
Statistical methods

PAI descriptive statistics was registered for each age group and sex. Mann--Whitney test was used to compare the mean PAIs between males and females. Linear, quadratic and log-linear statistical models were designed to investigate the progressive alterations of the PAIs with age. R^2 and Akaike Information Criterion were considered for choosing a single model that better described the facial development (YANG, 2005).

Additionally, the PAIs were investigated separately based on their contribution to the quadratic statistical model. Next, they were ranked based on their metric variability according to sex. Statistical analyses were performed with R (The R Foundation, Vienna, Austria) software package with significance level set at 5% and confidence interval of 95%.

Additionally, diagrams of the face were designed using the PAIs in order to represent the facial growth in relation to the regression curves obtained from the best statistical model. Figure 3 shows ten measurements that better illustrate the human face and its variation over the time were chosen, six of them were related to horizontal distances (facial width) and four to vertical distances (facial height). The Midnasal (mid) landmark was used in replacement of Glabella (g) and Nasion (n) as a fixed point in y axis (anchor point) because it was easier to locate in frontal images of the face. In order to design the diagrams of the face, standard photographs of females and males at the age of 2 years were used as baseline. From the baseline, cumulative percentages of growth within intervals of two years were multiplied – generating diagrams separately for females and males.

Figure 3 – Measurements taken from the human face to enable the simulation of age progression with cumulative growth

Number	Reference
1	al-al
2	ch-ch
3	ec_en (*mean right and left*)
4	en-en
5	go-go
6	zy-zy
7	mid-sn
8	mid-sto
9	mid-gn
10	li-ls

Legend: Four measurements were taken vertically and six were taken horizontally

Results

Intraclass Correlation Coefficient outcomes showed excellent intra- and inter-examiner reproducibility (>0.90, p<0.001).

The quadratic model figured as the best fit for describing the variations of the PAIs according to age, and sex. In females, the quadratic model reached R^2 values that ranged from 0.2% to 72.3% (mean: 52.14% ± 0.15), while the Akaike Information Criterion ranged from -39227.9 to 1399.84 (mean: -0.76 ± 2819.93). In males, the R^2 values with the same model ranged from 0.1% to 80.8% (mean: 60.87% ± 0.15), while the AIC values ranged from -38772.6 to 1450.17 (mean: 139.84 ± 2779.56) (Table 2).

Laíse Nascimento Correia Lima et al.

Table 2: Quality indicators of the three statistic models designed to describe facial growth in function of age distributed according to sex

Quality indicators	Females			Males		
	Model 1	Model 2	Model 3	Model 1	Model 2	Model 3
R^2 min. (%)	0.1	0.2	0.1	0	0.1	0
R^2 max. (%)	60.6	73.2	58.5	78	80.8	76.2
Mean R^2 (%)	41.49	52.14	40.27	58.53	60.87	57.48
Standard deviation	12.99	0.15	0.12	0.15	0.15	0.15
Median R^2 (%)	44	55	42	62	64	61
AIC min.	-39226.7	-39227.9	-3939.7	-38771.8	-38772.6	-41785
AIC max.	1443.73	1399.84	1449.42	1452.57	1450.17	1455.76
Mean AIC	140.80	-0.76	549.31	181.19	139.84	186.14
Standard deviation	2837.35	2819.93	3022.01	2784.71	2779.56	2990.65
Median AIC	555.66	373.94	576.96	562.56	513.32	576.5

R^2: Coefficient of determination; AIC: Akaike Information Criterion; Model 1: linear; Model 2: quadratic; Model 3: log-linear. R^2 and AIC values express the quality of each model for males and females. The first is directly proportional – the higher the value the better the model, while the second is the opposite – the lower the value the better the model.

PAI values were defined using the formula: $PAI = \beta\ Intercept + (real\ age \times \beta\ age) + (real\ age^2 \times \beta\ age^2)$. As an example, for a 10-year-old female, the value of PAI115, as shown in table 3, would be: PAI115 = 7.055 + (10 × 0.363) + (10^2 × (-0.009)). In this case, PAI 115 = 9.785.

In females and males, all the PAI showed statistically significant behavior with aging (p<0.05), except for the distances between the lateral (PAI 160) and medial (PAI 171) surface of the iris to the pupil in both sexes, and the distance from nasion to midnasal (PAI190) for males (p>0.05). Table 3 and figure 4 revealed that, in general, the height of the human face (PAI 115) figured as the PAI with highest alteration with age in the overall sample (p<0.05).

Table 3: Behavior of the photoanthropometric indicator (PAI) that showed the highest alteration in function of age in females and males

PAI	Factor	Females				Males			
		β	SE	CI (95%)	p	β	SE	CI95%	p
115	Intercept	7.055	0.081	[6.896; 7.215]	0.000	6.947	0.091	[6.770; 7.125]	0.000
	Age	0.363	0.014	[0.335; 0.391]	0.000	0.337	0.016	[0.305; 0.368]	0.000
	Age²	-0.009	0.001	[-0.01; -0.008]	0.000	-0.006	0.001	[-0.007; -0.005]	0.000

PAI: photoanthropometric indicators (the complete list with the description of each indicator may be available upon request); PAI 115: height of the face (showed more alterations with age); β: value of the intercept, age and age² in the quadratic equation from the statistical model; SE: standard error; CI: confidence interval range (95%); p: p-value with statistical significance set at 5%.

Figure 4: Representation of the photoanthropo-metric indicator (PAI) with the highest alteration over the time in females and males
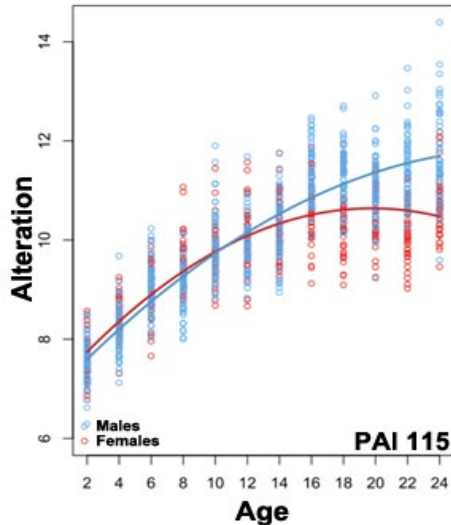
Legend: Height of the face (PAI 115) was the most altered PAI in function of age for females (red) and males (blue). This PAI is described as the relation between the distance of the landmarks glabella (g) and gnation (gn) in relation to the diameter of the iris.

In females, the five morphological measurements that had the most significant alterations were the height of the face (PAI 115: 0.363), followed by the distance from the chin to the medial surface of the iris (PAI 129: 0.334), the distance from the chin to the pupil (PAI 134: 0.332), the distance from the chin to the lateral surface of the iris (PAI 128: 0.330), and the distance from the chin to the ectocanthion (PAI 79: 0.329). According to table 4, in males, PAIs 115 (0.337), 129 (0.315) and 134 (0.311) repeated in the top, followed by the distance from the chin to the endocanthion (PAI 98: 0.307) and the distance from the chin to the lateral surface of the iris (PAI 128: 0.306).

Table 4: Top 5 photoanthropometric indicators (PAI) with the highest alterations with aging in females and males

Sex	PAI	Factor	β	SE	CI95%	p
F		Intercept	7.055	0.081	[6.896; 7.215]	0.000
	115	Age	0.363	0.014	[0.335; 0.391]	0.000
		Age²	-0.009	0.001	[-0.01; -0.008]	0.000
		Intercept	6.302	0.077	[6.152; 6.453]	0.000
	129	Age	0.334	0.013	[0.308; 0.36]	0.000
		Age²	-0.009	0.001	[-0.01; -0.008]	0.000
		Intercept	6.441	0.076	[6.291; 6.59]	0.000
	134	Age	0.332	0.013	[0.306; 0.359]	0.000
		Age²	-0.008	0.000	[-0.009; -0.007]	0.000
		Intercept	6.612	0.076	[6.463; 6.76]	0.000
	128	Age	0.330	0.013	[0.304; 0.356]	0.000
		Age²	-0.008	0.000	[-0.009; -0.007]	0.000
		Intercept	6.709	0.075	[6.563; 6.855]	0.000
	79	Age	0.329	0.013	[0.303; 0.355]	0.000
		Age²	-0.008	0.000	[-0.009; -0.007]	0.000
M		Intercept	6.947	0.091	[6.77; 7.125]	0.000
	115	Age	0.337	0.016	[0.305; 0.368]	0.000
		Age²	-0.006	0.001	[-0.007; -0.005]	0.000
		Intercept	6.204	0.085	[6.037; 6.372]	0.000
	129	Age	0.315	0.015	[0.285; 0.345]	0.000
		Age²	-0.006	0.001	[-0.007; -0.004]	0.000
		Intercept	6.352	0.085	[6.186; 6.517]	0.000
	134	Age	0.311	0.015	[0.281; 0.341]	0.000
		Age²	-0.005	0.001	[-0.007; -0.004]	0.000
		Intercept	5.880	0.084	[5.715; 6.045]	0.000
	98	Age	0.307	0.015	[0.278; 0.337]	0.000
		Age²	-0.005	0.001	[-0.007; -0.004]	0.000
		Intercept	6.534	0.084	[6.37; 6.698]	0.000
	128	Age	0.306	0.015	[0.277; 0.335]	0.000
		Age²	-0.005	0.001	[-0.006; -0.004]	0.000

F: females; M: males; PAI: photoanthropometric indicators (the complete list with the description of each indicator may be available upon request); PAI 115: height of the face; PAI 129: distance from the chin to the medial surface of the iris; PAI 134: distance from the chin to the pupil; PAI 128: distance from the chin to the lateral surface of the iris; PAI 79: distance from the chin to the ectocanthion; PAI 98: distance from the chin to the endocanthion; □: value of the intercept, age and age² in the quadratic equation from the statistical model; SE: standard error; CI: confidence interval range (95%); p: p-value with statistical significance set at 5%.

Table 5 is provided as a tool for practical simulation of facial growth. Specifically, this table shows the cumulative and gradual growth of the ten most significant morphological measurements in females and males from 2 to 24 years of age. In females, the highest cumulative growth was observed in the height of the lips (PAI 177), which grew 77% from 2 to 24 years; while in males the distance from the midnasal to the gnathion landmarks (PAI 132) showed the highest growth rate: 60% from 2 to 24 years – illustrated in figure 5.

Table 5: Top 10 morphological structures with the highest cumulative and gradual growth rates from 2- to 24-year-old females and females

Sex	PAI	2	4	6	8	10	12	14	16	18	20	22	24
F	0	0	5(+5)	9(+4)	12(+3)	15(+3)	17(+2)	19(+2)	20(+1)	20*	20	20	20
	27	0	9(+9)	17(+8)	23(+6)	29(+6)	33(+4)	36(+3)	39(+3)	40(+1)	40*	40	40
	76	0	5(+5)	9(+4)	12(+3)	14(+2)	16(+2)	17(+1)	17*	17	17	17	17
	96	0	4(+4)	7(+3)	10(+3)	12(+2)	14(+2)	14*	14	14	14	14	14
	138	0	4(+4)	8(+4)	11(+3)	14(+3)	16(+2)	18(+2)	19(+1)	20(+1)	20*	20	20
	192	0	9(+9)	17(+8)	23(+6)	28(+5)	32(+4)	35(+3)	37(+2)	37*	37	37	37
	193	0	8(+8)	14(+6)	20(+6)	24(+4)	28(+4)	30(+2)	32(+2)	33(+1)	33*	33	33
	132	0	8(+8)	16(+8)	22(+6)	27(+5)	32(+5)	35(+3)	38(+3)	39(+1)	40(+1)	40*	40
	177	0	11(+11)	22(+11)	31(+9)	40(+9)	48(+8)	55(+7)	61(+6)	66(+5)	71(+5)	74(+3)	77(+3)*
	207	0	4(+4)	7(+3)	9(+2)	12(+3)	13(+1)	15(+2)	15*	15	15	15	15
M	0	0	6(+6)	12(+6)	17(+5)	23(+6)	27(+4)	32(+5)	36(+4)	40(+4)	43(+3)	46(+3)	49(+3)*
	27	0	7(+7)	13(+6)	19(+6)	25(+6)	29(+4)	34(+5)	37(+3)	40(+3)	43(+3)	45(+2)	47(+2)*
	76	0	3(+3)	6(+3)	8(+2)	10(+2)	11(+1)	12(+1)	13(+1)	14(+1)	14*	14	14
	96	0	4(+4)	8(+4)	11(+3)	14(+3)	17(+3)	20(+3)	22(+2)	23(+1)	25(+2)	26(+1)	26*
	138	0	5(+5)	9(+4)	13(+4)	17(+4)	21(+4)	25(+4)	28(+3)	31(+3)	34(+3)	37(+3)	39(+2)*
	192	0	8(+8)	16(+8)	23(+7)	29(+6)	35(+6)	40(+5)	44(+4)	48(+4)	51(+3)	54(+3)	56(+2)*
	193	0	7(+7)	13(+6)	19(+6)	24(+5)	28(+4)	32(+4)	35(+3)	38(+3)	40(+2)	42(+2)	43(+1)*
	132	0	9(+9)	16(+7)	24(+8)	30(+6)	36(+6)	42(+6)	47(+5)	51(+4)	54(+3)	57(+3)	60(+3)*
	177	0	14(+14)	26(+12)	36(+10)	44(+8)	51(+6)	55(+4)	58(+3)	58*	58	58	58
	207	0	3(+3)	5(+2)	8(+3)	11(+3)	13(+2)	16(+3)	18(+2)	20(+2)	22(+2)	24(+2)	26(+2)*

F: females; M: males; PAI: photoanthropometric indicators; Cumulative (out of parentheses) and within-two-years gradual (in parentheses) growth rates expressed in percentage values (%); *: Facial structures signaling towards complete development.

Figure 5: Diagrams of the cumulative facial growth in females and males
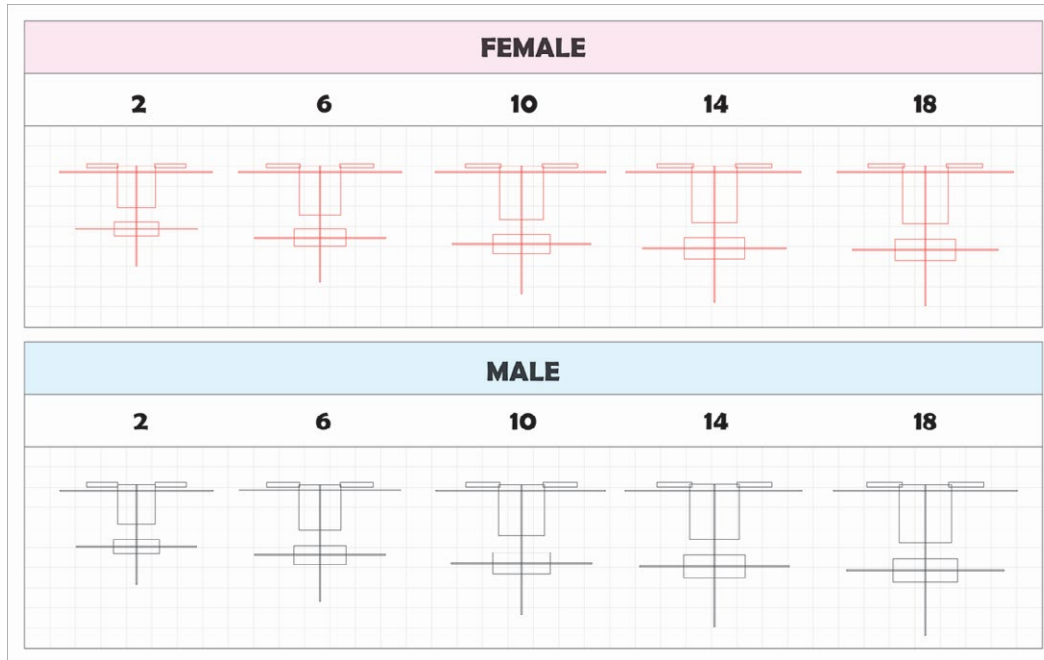
Legend: The diagrams of facial growth in females and males express the cumulative growth observed from 2 to 18 years within time intervals of 4 years. While the facial representations are realistic in the childhood and adolescence, non-realistic representations with a disproportional growth of the lower third of the face are shown around the age of 18. This phenomenon is generated by limitations inherent to the quadratic modeling and raises a flag for caution on the application of quadratic models for studying the dynamics of human facial growth in subadults.

Discussion

Studies about human facial aging may be performed in many fields of science to understand the phenotypic expression of gene polymorphisms (MARTINELLI *et al.,* 2016), to establish treatment plans for surgeries (HSIEH; DEDHIA; TOLLEFSON, 2018), to screen morphological alterations manifested in the oral cavity and the adjacent bones during life (SOUZA-SILVA *et al.*, 2018), and to provide morphological information in forensic investigations (OETTER; DEMETER; L'ABBÉ, 2016;

WÄRMLÄNDER *et al.*, 2019). However, the outcomes of predicting facial aging in practice depend on the available and applied methods. This study combined photoanthropometry and quadratic statistical modeling for the extraction and treatment of facial morphological data. The proposed methodological approach was able to describe the facial morphological alterations of female and male Brazilian subjects over the time.

The photoanthropometric approach used in the present study was founded on the projection of facial ratios based on the diameter of the iris. The stability of the

iris enables a visualization of dynamics of the PAIs and their relative growth (MACHADO *et al.*, 2017). Consequently, reliable ratios of the facial morphological structures were obtained. Recent studies in the field also addressed the diameter of the iris as a reference measurement for calculating ratios of the human face (MACHADO *et al.*, 2017; BORGES *et al.*, 2018). In these studies, the human face was mapped with a considerably lower quantity of measurements (n=10). Differently, the present study performed a deeper investigation of the morphology of the human face by analyzing the information from 208 measurements. In practice, the increase in the quantity of measurements allows a more detailed simulation of facial aging and a better understanding of growth dynamics.

An additional characteristic of the methods adopted in this study was the quality-control procedure established by comparing the performance of three different statistic models. The quadratic model reached better outcomes – with a mean coefficient of determination (R^2) of 52.14% (± 0.15) in females and 60.87% (± 0.15) in males. This finding may be justified by the fact that quadratic models describe better the outcomes that are not linearly distributed, such as the allometric human facial growth. "Allometry" is the term used to explain the harmonious growth of the normal human face within the different developmental timing of each facial structure (MANDARIN-DE-LACERDA, 1993).

Once the statistical model with better performance was selected, human facial growth outcomes were separately obtained based on sex. Females and males showed a prevalence of 99.04% and 100% of PAIs statistically associated with age ($p<0.05$), respectively. With the diameter of the iris as a reliable fixed reference in the human face, the behavior of the remaining 207 PAIs was assessed. The PAIs with the most evident morphological alteration over the time were those related to the vertical growth of the human face, especially the ratios that involved distances from the gnathion landmark (in the chin region) to the glabella, the eyes and the midnasal landmarks. Similarly, studies in the past described the facial growth in a fourth degree polynomial equation and showed that the vertical height of the human face may be associated with the mandibular plane (e.g. growth of the anterior height of the human face influences the mandibular plane) (VAN DER BEEK, HOEKSMA; PRAHL-ANDERSEN, 1991). Despite the strong connection with a clinical application in Plastic and Maxillofacial Surgery, the outcomes obtained in the past and in the present are not properly comparable because in the past longitudinal analysis were performed by landmarking bone references. In the present study, facial soft tissues are also taken into account, especially because they play an important part in simulations of age progression.

The analyses based on sex revealed that growth in females manifests earlier than males (Table 4). Figure 4 shows that

the height of the female face triggers a stronger development around the age of 11, while in males the ascending curve is more evident around the age of 14. This outcome is in accordance with the consolidated scientific literature on pubertal growth spurt (SOLIMAN *et al.,* 2014). Finally, it must be noted that growth is a quantifiable phenomenon that may be positive (increase in size) or negative (decrease in size) (MOSS, 1964). This study sampled a population of individuals that were in a young age range. Consequently, they may not express high negative values in growth as those expected in older ages (e.g. because of the decrease in muscular tissue). For this reason, specific PAIs do not show a descending (negative) curve in size.

In order to enable a better understanding of facial growth, ten PAIs ranked with the most evident alterations over the time were explored in table 5. In this table, the cumulative growth rates of facial ratios were provided for females and males from 2 to 24 years of age. Additionally, the gradual growth within an interval of two years was also reported and distributed based on sex. However, it is important to highlight that because of the inherent limitations of statistical modeling facial growth data is treated and expressed as a continuous phenomenon even in the early adulthood. Figure 5 illustrates this limitation by showing non-realistic representations of the predicted facial growth in females and males around the age of 18. More specifically, an overestimated growth

of the lower third of the human face is manifested. In practice, these outcomes indicate that photoanthropometry combined with quadratic modeling may be used for understanding facial growth patterns in health sciences, but may not be accurately enough to support criminal investigations in the forensic sciences. A clear application of the technique and statistical modeling, however, is in the field of human growth and aging (GONZALES; MACHADO; MICHEL-CROSATO, 2020). Understanding how the morphology of the human face changes over time is important to improve the prediction of orthopedic and orthodontic treatment, the establish treatment plan for maxillofacial surgeries, the understand patient's decision for orofacial aesthetics and to support the treatment of pediatric patients on follow-up sessions for body growth. Additionally, when facial aging is analyzed from the perspective of body growth, several applications emerge especially those related to understanding the abnormal development of the human body. The present study depicted the normal growth curve of male and females faces from a large and standardized sample. Comparisons of patients' development with the present facial growth and aging pattern might be interesting to investigate if abnormal morphological changes are expected or not.

Future studies in the field should investigate different populations in order to enable the extrapolation of the present outcomes worldwide. Statistic

approaches should include different data modeling, such as non-linear equations, to explore the behavior of the PAIs from a different perspective. Moreover, longitudinal studies are encouraged for a more realistic assessment of the development of the human face.

Conclusion

This study provided scientific evidence to support to use of photoanthropometric analysis and quadratic modeling to describe the dynamics of facial growth and aging from child- to adulthood. This approach can be used in studies dedicated to understand the growth and aging pattern of Brazilians. In particular, information of growth and aging is useful to enable optimal treatment plan, namely orthopedics, orthodontics, pediatrics, maxillofacial surgery and forensics. From a practical perspective, growth patterns of children and young adults could be compared to the pattern of facial growth and aging showed from the Brazilian faces sampled in this study.

Acknowledgements

A dinâmica do envelhecimento facial por meio de análise fotoantropométrica e modelagem quadrática da infância à fase adulta – um estudo multicêntrico

Resumo

Este estudo objetivou analisar a dinâmica do envelhecimento facial por meio de fotografias de indivíduos em diferentes grupos etários a fim de se estabelecer um padrão da maturação facial. A amostra consistiu de fotografias digitais obtidas padronizadamente de 1273 brasileiros com idades entre 2 e 24 anos igualmente distribuídos por sexo em doze grupos (2, 4, 6, 8, 10, 12, 14, 16, 18, 20, 22 e 24 anos). O software SAFF-2D® (Sistema de Análise Facial Forense, Polícia Federal Brasileira, Brasil) foi utilizado para a marcação de 28 pontos de referências em cada imagem. Duzentas e oito medidas foram calculadas. Indicadores fotoantropométricos (IFA) da anatomia facial foram obtidos com base em uma referência fixa (diâmetro da íris). Os modelos estatísticos linear não transformado, quadrático e log-linear foram testados para investigar a melhor abordagem para descrever a dinâmica do envelhecimento facial em mulheres e homens. A modelagem quadrática atingiu os melhores resultados para mulheres (R^2 <73.2%, média: 52.14% ± 0.15) e homens (R^2 <80.8%, média: 60.87% ± 0.15). A maioria dos IFA (>99.04%) foi estatisticamente associada com a idade em mulheres e homens ($p<0.05$). Alterações faciais verticais foram as mais evidentes com o envelhecimento, em especial a al-

tura da face (p<0.05). A extração e trata-
mento de dados realizados neste estudo
demonstraram que a fotoantropometria e
a modelagem quadrática compuseram a
melhor abordagem para descrever a dinâ-
mica do crescimento facial envelhecido da
infância à fase adulta.

Palavras-chave: Envelhecimento; Anato-
mia; Antropologia; Medicina Legal; Odon-
tologia Legal.

References

BICALHO, G. C.; ALVES, M. C. A.; PORTO,
L. F.; MACHADO, C. E. P.; VIDAL, F. de B.
Solving the facial growth problem in the
biometric face recognition using photo-an-
thropometric ratios by iris normalization.
*International Workshop on Biometrics and
Forensics*, Piscataway, v. 1, n. 1, p. 1-6, 2018.
Doi: 10.1109/IWBF43282.2018

BISHARA, S. E. Facial and dental chan-
ges in adolescents and their clinical im-
plications. *Angle Orthodontist*, Apple-
ton, n. 70, n. 6, p. 471-483, 2000. Doi:
10.1043/0003-3219(2000)070<0471:FAD-
CIA>2.0.CO;2

BORGES, D. L.; VIDAL, F. B.; FLORES, M.
R. P.; MELANI, R. F. H.; GUIMARÃES, M.
A.; MACHADO, C. E. Photoanthropometric
face iridial proportions for age estimation:
An investigation using features selected
via a joint mutual information criterion.
Forensic Science International, Lausanne,
v. 284, n. 1, p. 9-14, 2018. Doi: 10.1016/j.
forsciint.2017.12.011

CATTANEO, C.; OBERTOVÁ, Z.; RATNAYA-
KE, M.; MARASCIUOLO, L.; TUTKUVIE-
NE, J.; POPPA, P.; GIBELLI, D.; GABRIEL,
P.; RITZ-TIMME, S. Can facial proportions
taken from images be of use for ageing in
cases of suspected child pornography? A
pilot study. *International Journal of Legal
Medicine*, Heidelberg, v. 126, n. 1, p. 139-144,
2012. Doi: 10.1007/s00414-011-0564-7

CATTANEO, C.; RITZ-TIMME, S.; GA-
BRIEL, P.; GIBELLI, D.; GIUDICI, E.;
POPPA, P.; NOHRDEN, D.; ASSMANN,
S.; SCHMITT, R.; GRANDI, M. The difficult
issue of age assessment on pedo-pornogra-
phic material. *Forensic Science International*,
Lausanne, v. 138, n. 1-3, p. 21-24, 2009. Doi:
10.1016/j.forsciint.2008.09.005

CHARMAN, S. D.; CAROL, R. N. Age-pro-
gressed images may harm recognition of
missing children by increasing the number
of plausible targets. *Journal of Applied Re-
search in Memory Cognition*, Amsterdam,
v. 1, n. 3, p. 171-178, 2012. Doi: 10.1016/j.
jarmac.2012.07.008

DAVIS, J. P.; VALENTINE, T.; DAVIS, R. E.
Computer assisted photo-anthropometric
analyses of full-face and profile facial images.
Forensic Science International, Lausanne, v.
200, n. 1-3, p. 165-176, 2010. Doi: 10.1016/j.
forsciint.2010.04.012.

ENLOW, D. H. Facial Growth. Philadelphia:
Saunders, 1990.

ERICKSON, W. B.; LAMPINEN, J. M.;
FROWD, C. D.; MAHONEY, G. When age-
-progressed images are unreliable: The roles
of external features and age range. *Science
& Justice*, Harrogate, v. 57, n. 2, p. 136-143,
2017. Doi: 10.1016/j.scijus.2016.11.006

FLORES, M. R. P.; MACHADO, C. E. P.
Manual of facial photoanthropometry: land-
marks in frontal view from visual references.
Brasília: National Institute of Criminalistics,
2017.

FLORES, M. R. P.; MACHADO, C. E. P.;
GALLIDABINO, M. D.; ARRUDA, G. H. M.
DE; SILVA, R. H. A. DA; VIDAL, F. B. DE;
MELANI, R. F. H. Comparative assessment
of a novel photo-anthropometric landmark-
positioning approach for the analysis of
facial structures on two-dimensional images.
Journal of Forensic Sciences, Chicago, v. 64,
n. 3, p. 828-838, 2019. Doi: 10.1111/1556-
4029.13935

GONZALES, P. S.; MACHADO, C. E. P.; MICHEL-CROSATO, E. Analysis of neoclassical facial canons for Brazilian white young adults and comparison with North American Caucasian population. *The Journal of Craniofacial Surgery,* Ontario, v. 31, n. 5, p. e432-e435, 2020. Doi: 10.1097/SCS.0000000000006339

HSIEH, T. Y.; DEDHIA, R.; TOLLEFSON, T. T. Cleft rhinoplasty: Strategies for the multiply operated nose. *Facial Plastic Surgery,* New York, v. 34, n. 3, p. 290-297, 2018. Doi: 10.1055/s-0038-1653986

ISÇAN, M. Y.; HELMER, R. P. Forensic analysis of the skull. New York: Wiley-Liss, 1993.

KLEINBERG, K. F.; VANEZIS, P.; BURTON. A. M. Failure of anthropometry as a facial identification technique using high quality photographs. *Journal of Forensic Sciences*, Chicago, v. 52, n. 4, p. 779-783, 2007. Doi: 10.1111/j.1556-4029.2007.00458.x

KOUDELOVÁ, J.; DUPEJ. J.; BR□□EK, J.; SEDLAK, P.; VELEMÍNSKÁ, J. Modeling of facial growth in Czech children based on longitudinal data: Age progression from 12 to 15 years using 3D surface models. *Forensic Science International*, Lausanne, v. 248, n. 1, p. 33-40, 2015. Doi: 10.1016/j.forsciint.2014.12.005

LAMPINEN, J.; ARNAL, J. D.; ADAMS, J.; COURTNEY, K.; HICKS, J. L. Forensic age progression and the search for missing children. *Psychology, Crime & Law*, Milton Park, v. 18, n. 4, p. 405-415, 2012. Doi: 10.1080/1068316X.2010.499873

LINDSAY, K. E.; RÜHLI, F. J.; DELEON, V. B. Revealing the face of an ancient Egyptian: synthesis of current and traditional approaches to evidence-based facial approximation. *Anatomical Record,* Hoboken, v. 298, n. 6, p. 1144-1161, 2015. Doi: 10.1002/ar.23146

MACHADO, C. E. P.; FLORES, M. R. P.; LIMA, L. N. C.; TINOCO, R. L. R.; FRANCO, A.; BEZERRA, A. C. B.; EVISON, M. P.;

GUIMARÃES, M. A. A new approach for the analysis of facial growth and age estimation: Iris ratio. *PLoS One*, San Francisco, v. 12, n. 1, p. e0180330-0180330, 2017. Doi: 10.1371/journal.pone.0180330

MANDARIN-DE-LACERDA, C. A.; URANIA-ALVES, M. Growth allometry of the human face: analysis of the osseous component of the mid and lower face of Brazilian fetuses. *Annals of Anatomy*, New York, v. 175, n. 5, p.475-479, 1993. Doi: 10.1016/S0940-9602(11)80119-6

MARTINELLI, M.; GIRARDI, A.; CURA, F.; NOURI, N.; PINTO, V.; CARINCI, F.; MORSELLI, P. G.; SALEHI, M., SCAPOLI, L. Non-syndromic cleft lip with or without cleft palate in Asian populations: Association analysis on three gene polymorphisms of the folate pathway. *Archives of Oral Biology*, Oxford, v. 61, n. 1, p. 79-82, 2016. Doi: 10.1016/j.archoralbio.2015.10.019

MORETON, R.; MORLEY, J. Investigation into the use of photoanthropometry in facial image comparison. *Forensic Science International*, Lausanne, v. 212, n. 1-3, p. 231-237, 2011. Doi: 10.1016/j.forsciint.2011.06.023

MOREWITZ, S. J.; COLLS, C. S. Handbook of missing persons. Cham: Springer International Publishing, 2016.

MOSS, M.L. Vertical growth of the human face. *American Journal of Orthodontics and Dentofacial Orthopedics*, Amsterdam, v. 50, n. 5, p. 359-376, 1964. Doi: 10.1016/0002-9416(64)90176-9

OETTER, A. C.; DEMETER, F. P.; L'ABBÉ, E. N. Ancestral variations in the shape and size of the zygoma. *Anatomical Record*, Hoboken, v. 300, n. 1, p. 196-208, 2017. Doi: 10.1002/ar.23469.

RAFAI, N.; LEMOS, M.; KENNES, L. N.; HAWARI, A.; GERHARDT-SZÉP, S.; CLASSEN-LINKE, I. Anatomy meets dentistry! Linking anatomy and clinical practice in the preclinical dental curriculum. *BMC Me-*

dical Education, London, v. 16, n. 1, p. 305-305, 2016. Doi: 10.1186/s12909-016-0825-8

RATNAYAKE, M.; OBERTOVÁ, Z.; DOSE, M.; GABRIEL, P.; BRÖKER, H. M.; BRAUCKMANN, M.; BARKUS, A.; RIZGELIENE, R.; TUTKUVIENE, J.; RITZ-TIMME, S.; MARASCIUOLO, L.; GIBELLI, D.; CATTANEO, C. The juvenile face as a suitable age indicator in child pornography cases: a pilot study on the reliability of automated and visual estimation approaches. *International Journal of Legal Medicine*, Heidelberg, v. 128, n. 5, p. 803-808, 2014. Doi: 10.1007/s00414-013-0875-y

RICANEK, K.; BOONE, E. The effect of normal adult aging on standard PCA face recognition accuracy rates. *IEEE International Joint Conference on Neural Networks*, Piscataway, v. 1, n. 1, p. 2018-2023, 2005. Doi: 10.1109/IJCNN.2005.1556210

RIGHI, G.; PEISSIG, J. J.; TARR, M. J. Recognizing disguised faces. *Visual Cognition,* Milton Park, v. 20, n. 2, p. 143-169, 2012. Doi: 10.1080/13506285.2012.654624

SCANDRETT, C. M.; SOLOMON, C. J.; GIBSON, S. J. A person-specific, rigorous aging model of the human face. *Pattern Recognition Letters*, Amsterdam, v. 27, n. 15, p. 1776-1787, 2006. Doi: 10.1016/j.patrec.2006.02.007

SOLIMAN, A.; SANCTIS, V. DE; ELALAILY, R.; BEDAIR, S. Advances in pubertal growth and factors influencing it: Can we increase pubertal growth? *Indian Journal of Endocrinology and Metabolism,* Mumbai, v. 18, n. 1, p. s53-62, 2014. Doi: 10.4103/2230-8210.145075

SOUZA-SILVA, B. N.; VIEIRA, W. DE A.; BERNARDINO, Í. DE M.; BATISTA, M. J.; BITTENCOURT, M. A. V.; PARANHOS, L. R. Non-syndromic tooth agenesis patterns and their association with other dental anomalies: A retrospective study. *Archives of Oral Biology*, Oxford, v. 96, n. 1, p. 26-32, 2018. Doi: 10.1016/j.archoralbio.2018.08.014

TAYLOR, K. T. Forensic Art and Illustration. Boca Raton: CRC Press, 2000.

TEMPORINI, H. Child pornography and the internet. *The Psychiatry Clinics of North America*, Philadelphia, v. 35, n. 4, p. 821-835, 2012. Doi: 10.1016/j.psc.2012.08.004

TURK, M.; PENTLAND, A. Eigenfaces for recognition. *Journal of Cognition Neurosciences,* Cambridge, v. 3, n. 1, p. 71-86, 1991. Doi: 10.1162/jocn.1991.3.1.71

VALENTINE, T. Face-space models of face recognition. In: WENGER, M. J.; TOWNSEND, J. T. (Org.). Computational, geometric, and process perspectives on facial cognition - contexts and challenges. Hillsdale: Lawrence Erlbaum Associates, 2001. p. 83-113.

VAN DER BEEK, M. C. J.; HOEKSMA, J. B.; PRAHL-ANDERSEN, B. Vertical facial growth: a longitudinal study from 7 to 14 years of age. *European Journal of Orthodontics*, Oxford, v. 13, n. 3, p. 202-208, 1991. Doi: 10.1093/ejo/13.3.202.

VON ELM, E.; ALTMAN, D. G.; EGGER, M.; POCOCK, PETER, S. J.; GØTZSCHE, C.; VANDENBROUCKE, J. P. The strengthening the reporting of observational studies in epidemiology (STROBE) statement: guidelines for reporting observational studies. *Journal of Clinical Epidemiology*, Oxford, v. 61, n. 4, p. 344-349, 2008. Doi: 10.1016/j.jclinepi.2007.11.008.

WÄRMLÄNDER, S. K. T. S.; GARVIN, H.; GUYOMARC'H, P.; PETAROS, A.; SHOLTS, S. B. Landmark typology in applied morphometrics studies: what's the point? *Anatomical Record*, Hoboken, v. 302, n. 7, p. 1144-1153, 2019. Doi: 10.1002/ar.24005

WILKINSON C.; RYNN, C. Craniofacial identification. Cambridge: Cambridge University Press, 2012.

XU, C.; MAKIHARA, Y.; YAGI, Y.; LU, J. Gait-based age progression/regression: a baseline and performance evaluation by age

group classification and cross-age gait identification. *Machine Vision and Applications*, New York, v. 30, n. 1, p. 629-644, 2019. Doi: 10.1007/s00138-019-01015-x

YANG, Y. Can the strengths of AIC and BIC be shared? A conflict between model identification and regression estimation. *Biometrika*, Oxford, v. 92, n. 4, p. 937-950, 2005.

ZENG, J.; MA, X.; ZHOU, K. Photo-realistic face age progression/regression using a single generative adversarial network. *Neurocomputing,* Amsterdam, v. 366, n. 13, p. 295-204., 2019. Doi: 10.1016/j.neucom.2019.07.085

Corresponding author

Laíse Nascimento Correia Lima
Departamento de Odontologia I
Universidade Federal do Maranhão, Brasil
Av. dos Portugueses, s/n – Bacanga
EP: 65.080-805, São Luís, MA, Brasil
Phone: + 55 61 98365-9890
E-mail: laiselima@msn.com